unWISE Bitmasks: Bit Definitions and Methodology

Aaron Meisner, 12/2018

In Meisner et al. (2017a) we first introduced simplistic bright star masks to the set of unWISE coadd data products. These masks exist as a set of 18,240 images which together cover the entire sky. There is one unWISE bitmask image per unWISE tile footprint, combining artifact flagging information about the W1 and W2 bands into a single file. Currently, the unWISE bitmasks do not address the W3 or W4 bands, although extending them to do so is conceivable.

The original unWISE bitmasks from Meisner et al. (2017a) contained only four bits. For the sake of several research projects, particularly CatWISE (Eisenhardt et al., in prep.) and the unWISE Catalog (Schlafly et al., in prep.), the masks have become far more sophisticated since our initial Meisner et al. (2017a) versions were published. The total number of mask bits has increased from 4 to 31, and much more work has gone into making sure that the masking behaves properly as a function of sky location (e.g., at low Galactic latitude and high ecliptic latitude). This document contains an up-to-date explanation of the meanings of all mask bits, how the different bits are related to one another, and the detailed procedure for creating each mask bit.

Currently, the goal of the unWISE bitmasks is to provide a general purpose artifact flagging capability comparable to that of the WISE team's "CC flags", which were generated by a module called ARTID[1]. The unWISE bitmasks are also constructed with particular emphasis on enabling rare object searches ($\lesssim 1$ per 500 deg^2). Most but not all of the unWISE mask bits are associated with artifacts from bright stars (see Table 1). The unWISE bitmasks are integer-valued and populated with sums of powers of 2, such that a particular bit can be isolated by taking the bitwise AND between the mask image and the desired power of 2. The mask bit definitions in Table 1 are also documented in the FITS header of each unWISE bitmask image.

The unWISE bitmasks are optimized for catalogs that use detailed "pixelized" WISE PSF modeling and have a flexible WISE sky background model. To the extent that these capabilities are not implemented in a given WISE catalog's construction, the unWISE bitmasks may underflag features such as diffraction spikes and background level variations due to scattered light. Some artifacts are assigned separate unWISE mask bits for northward versus southward scan directions; this may be useful for time domain applications.

1 Bright source sample

A first step toward creating the unWISE bitmask images is defining a sample of sources which are sufficiently bright to potentially cause artifacts that require flagging. In Meisner et al. (2017a), we obtained such a sample via a simple full-sky query of the AllWISE catalog. Specifically, we selected all AllWISE sources with `w1mpro` < 9.5 (`w2mpro` < 8.3) in W1 (W2). We use Vega magnitudes and fluxes throughout this document unless otherwise noted. The equivalent thresholds in AB are 12.2 (11.64) in W1 (W2). Over the entire sky, this yields samples of 6,365,819 (2,221,020) sources in W1 (W2), with the density of such sources increasing dramatically near the Galactic plane. At $|b_{gal}| > 18^\circ$ (high enough Galactic latitude to fall within DESI's footprint), this bright source sample has on average $\sim$29 ($\sim$11) sources per deg^2 in W1 (W2).

Unfortunately, the AllWISE catalog lacks entries for some bright stars, and can report highly inaccurate (or "null") fluxes for some exceptionally bright objects that have far exceeded the WISE saturation threshold. To remedy this, the WISE team's ARTID artifact flagging module employed a custom "Bright Star List" that merged information from WISE itself, 2MASS, and even IRAS[2]. Here, we take a similar approach to enhancing our AllWISE-based bright source list, but using only 2MASS K_S magnitudes in a simplistic manner.

To merge 2MASS K_S information into our AllWISE-based bright source list, we begin by selecting all 68,661 2MASS sources with $K_S < 5$. We then cross-match this 2MASS K_S bright sample with our AllWISE sample, using a 15″ radius. This radius is chosen to allow for matching of stars with proper motions of up to $|\mu| \approx 1.5''$/yr given the $\sim$10 year AllWISE-2MASS time baseline. This proper motion threshold seems reasonable given that only $\sim$275 sources with $|\mu| > 1.5''$/yr are known, many of which (brown dwarfs, white dwarfs) are not sufficiently bright in W1 or W2 to require masking. For cases where an AllWISE bright source has a 2MASS $K_S < 5$ match within 15″, we

[1] `http://wise2.ipac.caltech.edu/docs/release/allsky/expsup/sec4_4g.html`; ARTID computes flags at the catalog level and did not produce image-level renderings like those of the unWISE bitmasks.

[2] `http://wise2.ipac.caltech.edu/docs/release/allsky/expsup/sec4_4g.html#bright_source_list`

Table 1: Description of unWISE mask bits.

Bit	Description
0	W1 bright star, southward scan
1	W1 bright star, northward scan
2	W2 bright star, southward scan
3	W2 bright star, northward scan
4	W1 bright star saturation
5	W2 bright star saturation
6	center of pixel not primary
7	W1 bright star, centroid off edge
8	W2 bright star, centroid off edge
9	resolved galaxy
10	big object (LMC, SMC, M31)
11	W2 optical ghost, southward scan
12	W2 optical ghost, northward scan
13	W1 first latent, southward scan
14	W1 first latent, northward scan
15	W2 first latent, southward scan
16	W2 first latent, northward scan
17	W1 second latent, southward scan
18	W1 second latent, northward scan
19	W2 second latent, southward scan
20	W2 second latent, northward scan
21	may contain W1 bright star centroid
22	may contain W2 bright star centroid
23	AllWISE-like W1 circular halo
24	AllWISE-like W2 circular halo
25	W1 optical ghost, southward scan
26	W1 optical ghost, northward scan
27	PSF-based W1 diffraction spike
28	PSF-based W2 diffraction spike
29	geometric W1 diffraction spike
30	geometric W2 diffraction spike

replace our bright source catalog's `w?mpro` magnitude with the 2MASS K_S magnitude, if $K_S <$ `w?mpro`. For 2MASS $K_S < 5$ sources with no AllWISE bright source match within $15''$ or a match at $>5''$ separation, we instantiate a new object in our WISE bright source list at the 2MASS object's position and with its `w?mpro` value set to the 2MASS K_S magnitude. In W1 (W2), 4,582 (877) bright sources have their WISE magnitudes replaced with 2MASS K_S, and an additional 2,767 (2,414) WISE bright source sample entries are instantiated based on 2MASS.

In the future we will investigate ways to more accurately predict W1 and W2 magnitudes of bright stars based on multi-band 2MASS JHK_S photometry, perhaps in combination with Gaia magnitudes and/or parallaxes. Also, given the availability of Gaia proper motions, improved 2MASS-AllWISE cross-matching could be enabled by propagating 2MASS positions to the AllWISE epoch. Lastly, unWISE coadds incorporate data spanning a considerable $\sim$8 year time period, so that one could imagine augmenting our WISE bright source list with motion information to instantiate multiple entries for bright sources that are moving very rapidly.

2 PSF model thresholding

Many of the unWISE mask bits are generated via a method that I refer to as "PSF model thresholding": on each tile's footprint in each band, we render a model image containing only objects from our bright source sample, then produce binary masks by flagging model image pixels brighter than a specified threshold as being "contaminated". Figure 1 illustrates an example of this methodology. The W1 and W2 PSF models themselves are shown in the left

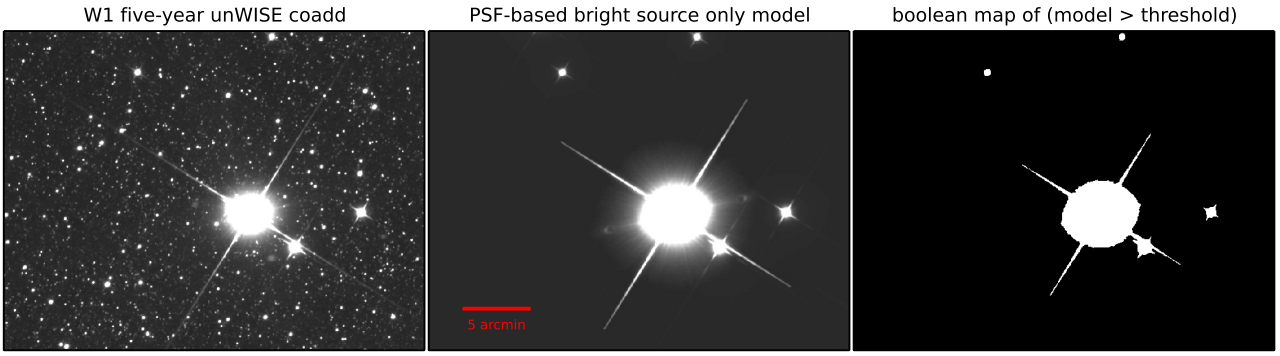

Figure 1: Schematic illustration of our PSF model thresholding procedure used in creating the unWISE bitmask images. Left: Portion of a five-year full-depth W1 unWISE coadd extracted from unWISE tile footprint 2415p106. The central, brightest source has AllWISE `w1mpro` ≈ 1.4. Middle: Bright source only model rendering of the same sky region, generated by combining the Meisner & Finkbeiner (2014) W1 PSF model, the unWISE coadd WCS, and our bright source list described in §1. Right: Bright source only model thresholded at 100 Vega nanomaggies per pixel to create a boolean bitmask, as we do when generating unWISE mask bits 0 and 1. The white regions represent pixels flagged as contaminated by bright sources.

column of Figure 2.

The key inputs to this procedure are the positions and fluxes from our bright source catalog (§1), and the PSF model used to render the bright star profiles. For this purpose, we employ the Meisner & Finkbeiner (2014) W1 and W2 PSF models. These PSF models natively exist in WISE detector coordinates, so we must perform several modifications before applying them to render models of unWISE coadds. The Meisner & Finkbeiner (2014) PSFs include terms that account for PSF variation as a function of position within the detector. Because we wish to render models of unWISE coadd images that sample many detector positions at each bright source's location, we begin by constructing a PSF in each band that averages over detector position. We then use the world coordinate system of each coadd footprint to rotate the averaged PSF such that it has an orientation matching that of the detector on the sky. Typically there are two such rotations for each unWISE tile footprint, corresponding to northward and southward WISE scans — these two rotations of the PSF differ by 180° from one another. At very high ecliptic latitude, each bright star's location samples a substantial range of approach angles toward the ecliptic pole, meaning that the simple approximation of two discrete scan directions with PSF orientations separated by 180° no longer suffices. Currently, the unWISE mask bits constructed via PSF model thresholding do not account for this effect, which is only relevant over a very small fraction of the sky. With the PSF model averaged and rotated, for each bright source, we scale the PSF amplitude according to its magnitude listed in our bright source catalog and add it to the model image at the appropriate location. With the bright star model images in hand for each unWISE tile footprint, scan direction, and band we can proceed to apply various thresholding criteria, thereby flagging several types of artifacts. Full details of these thresholding steps are provided in subsequent sections.

One major limitation of the PSF model thresholding approach is that such flagging is limited in angular extent by the size of the PSF model. The Meisner & Finkbeiner (2014) W1/W2 PSFs extend quite far into the wings, with sidelengths of $14.9'$ ($\sim$135 FWHM). Still, extremely bright stars can have diffraction spikes and "halos" reaching beyond the extent of our PSF models. Diffraction spikes become too long for the PSF models at parent magnitudes brighter than $\sim 5-6$. At $\sim 0-0.5$ mag, the circularly symmetric component of the PSF profile begins to extend beyond our PSF model. Therefore, we also produce geometric masks for diffraction spikes (§14) and bright source circular halos (§12), with radii that can extend far beyond the size of our PSF models.

3 Bits 0-3: bright star 'core and wings'

Bits 0-3 are the original four mask bits from the Meisner et al. (2017a) unWISE bitmasks. They can be thought of as flagging the $\sim$0.6% (0.4%) of pixels most strongly affected by nearby bright source profiles in high Galactic latitude sky regions. These masks were originally created to identify areas affected by difference imaging artifacts in

the Meisner et al. (2017b) analysis. Thus, these bits may provide sufficient bright star masking for unWISE-based difference imaging analyses, or other analyses in which the PSF modeling yields residuals comparably good to those from difference imaging.

Having rendered our bright source only model as described in §2 for the relevant band, scan direction and unWISE tile footprint, generating mask bits 0-3 amounts to simply thresholding on the model pixel values. Based on examination of typical extragalactic sky regions, we adopt the same baseline threshold in W1 and W2: $\Gamma_0 = 100$ nanomaggies per pixel. We then scale the brightness threshold (Γ) up with increasing source density, in attempt to avoid masking an excessive fraction of area at low Galactic latitude. To implement this scaling of Γ with source density, we begin by constructing a map of the number of Gaia DR2 (Gaia Collaboration 2018) sources per n_{side} = 32 HEALPix pixel. We interpolate over the raw Gaia sources counts in HEALPix pixels affected by small-scale source density spikes (e.g., globular clusters) and localized dust clouds. We then interpolate off of the resulting source density map at coordinates corresponding to the center of the unWISE tile footprint for which we are constructing a bitmask, and refer to the resulting value as n_{src} (units of Gaia sources per $n_{side} = 32$ HEALPix pixel). The threshold Γ in nmgy/pixel as a function of source density is then determined by:

$$\Gamma = \Gamma_0 + (max(n_{src}, 10^5) - 10^5) \times (\Gamma_{max} - \Gamma_0)/(n_{src,max} - 10^5) \quad (1)$$

So the threshold ramps linearly from its minimum value of Γ_0 to its peak value of Γ_{max} between $n_{src} = 10^5$ and $n_{src} = n_{src,max}$. Γ remains at its baseline value so long as $n_{src} < 10^5$, which is the case for $\sim$75% of the sky. n_{max} is 3.1×10^6 Gaia sources per $n_{side} = 32$ HEALPix pixel. Γ_{max} is 10,000 nmgy/pixel (9250 nmgy/pixel) in W1 (W2).

Bit 0 (1) marks pixels which have values larger than Γ in the southward (northward) scan W1 model rendering. The same holds for bits 2 and 3 in W2. In constructing each of bits 0-3, we also dilate the binary map of pixels above threshold by a 3×3 square kernel. We refer to these bits as 'core and wings' because they capture the cores of bright star profiles, extending somewhat out into the wings so as to also capture diffraction spikes and optical ghosts for sufficiently bright objects. The most noticeable scan direction dependence seen in bits 0-3 pertains to the W2 ghost location, appearing on opposite sides of the parent bright star in opposite scan directions.

Note that bits 0-3 mask regions containing the parent bright source centroids themselves. Also, bits 0-3 account properly for cases in which some portion of a parent bright source's PSF profile overlaps the tile under consideration despite the parent's centroid falling outside of the tile boundaries.

4 Bits 4-5: bright source saturation

PSF modeling of bright sources will be compromised by inclusion of saturated pixels near the profile core. To address this, unWISE mask bit 4 (5) marks "saturated" pixels in W1 (W2). Pixels flagged by bit 4 (5) are the subset of pixels flagged by bright source bits 0 OR 1 (2 OR 3) with model profile values which exceed thresholds of 85,000 (130,000) Vega nanomaggies in W1 (W2). Note that these per-band thresholds are fixed across the entire sky, with no spatial variation.

For the purposes of these unWISE mask bits, we have not intended to define the "saturation" threshold such that it truly corresponds to saturation of the WISE detectors. Instead, we are masking pixels which may be either fully saturated, potentially non-linear, or be bright enough to experience non-linearities to due interactions with outlier rejection during unWISE coaddition. At high Galactic latitude, the fraction of area masked by bit 4 (5) is 4.3×10^{-5} (3.0×10^{-5}).

5 Bit 6: center of pixel not primary

unWISE tile footprints are not mutually exclusive, and overlap by varying amounts depending on sky position. Typically, the overlap is $\sim 3'$ along each boundary. As a result, one may sometimes wish to determine the "best" unWISE tile to consult for a specific (RA, Dec) sky location given the multiple tiles available to choose from. There are different possible ways to define "best". Here we define the best unWISE tile for a given (RA, Dec) as the tile which maximizes the minimum distance of that (RA, Dec) from any tile edge. For each pixel center's location within a given tile, one can compute whether this tile is the best tile for that pixel's (RA, Dec), or instead whether that sky location would be better analyzed in some other tile. Pixels marked with the "center of pixel not primary" unWISE mask bit are sky locations that would be better analyzed in another tile. The region flagged by this bit is a border

along the edges of the tile, with a typical width of ∼35 pixels. This mask bit is the unWISE analog of the 2^0 mask bit in the DESI imaging `-maskbits` product.

6 Bits 7-8: contamination from bright source with centroid off tile edge

A bright source with PSF wings that contaminate an unWISE tile's footprint despite the bright source's centroid itself falling outside of the tile boundary can be problematic for image modeling analyses. For instance, the unWISE Catalog pipeline treats each unWISE tile footprint independently, detecting and modeling only those sources with centroids inside of the tile boundaries. As a result, the catalog creation process would by default be predisposed to model flux from the wings of off-edge bright sources as sums of large numbers of fainter point sources. To avoid this outcome, unWISE mask bits 7 and 8 flag pixels affected by bright stars with centroids outside of the tile's footprint. The unWISE Catalog pipeline recognizes these bits and uses them to preemptively make deblending less aggressive in the affected regions.

Bits 7-8 are based on bits 0-3 described in §3. For W1, if bit 0 and/or bit 1 is set and the parent bright star centroid is off the tile edge, then bit 7 is also set. For W2, if bit 2 and/or bit 3 is set and the parent bright star centroid is off the tile edge, then bit 8 is also set. Because bit 7 (8) combines bits 0-1 (2-3) in W1 (W2), information about scan direction is not retained in bits 7-8.

7 Bit 9: resolved galaxy

Certain image analyses may encounter problems in regions affected by resolved galaxies. For instance, the unWISE Catalog pipeline does not perform any galaxy model fitting, and by default deblends aggressively in attempt to explain all flux above background as a sum of point sources. Flagging of resolved galaxies allows unWISE Catalog deblending to be made less aggressive in these regions; this avoids shredding resolved galaxies into large numbers of point sources. For our purposes, resolved galaxies are those with sizes $\gtrsim 6.5''$, which is the approximate W1/W2 PSF FWHM.

To flag resolved galaxies, we use an early version of the Legacy Survey Large Galaxy Atlas[3] (LSLGA), produced by John Moustakas. This catalog contains ∼2.1 million galaxies with angular sizes of $d_{25} \gtrsim 7''$, a size threshold coincidentally well-matched to the WISE FWHM. We visually inspected the largest (in terms of angular size) 300 LSLGA galaxies, manually removing a small number of SDSS filter edge reflection artifacts and very low surface brightness dwarf galaxies, and also tweaking a few of the d_{25} parameters by eye. Based on this slightly modified LSLGA catalog, we used unWISE mask bit 9 to flag elliptical regions about each resolved galaxy, with the ellipse size set by d_{25} and the appropriate shape/orientation determined by the axis ratio and position angle. d_{25} is taken to be the major axis of the elliptical mask, as this visually appeared to work well. We masked circular regions in cases where position angles and/or axis ratios were not available. We also floored the b/a axis ratio at 0.5 to avoid overly line-like masked regions. The median per-tile fraction of area flagged by the resolved galaxy bit is 0.08%.

8 Bit 10: big object

This mask bit was inspired by (and largely copied from) the `big_obj` mask bit within the Schlegel et al. (1998; SFD) dust map data products. Its purpose is to flag regions affected by the LMC, SMC and M31. For the LMC and SMC, the unWISE big object mask bit is set for each pixel based on querying the SFD `big_obj` mask bit at that pixel center's (RA, Dec) coordinates. For M31, we use an elliptical mask with $a = 100'$, $a/b = 2.82$, and position angle of 35° east of north. This position angle was chosen in order to best cover M31's outskirts.

9 Bits 11-12 and 25-26: optical ghost

Bright source ghosts are captured by the Meisner & Finkbeiner (2014) PSF models (see Figure 2). As a result, we can employ our PSF model thresholding approach in order to specially flag regions affected by ghosts, making use of the thresholding criterion defined in §3. When rendering the same bright source only model used to create bits

[3] `https://github.com/moustakas/LSLGA`. The LSLGA is based on HyperLeda (Makarov et al. 2014).

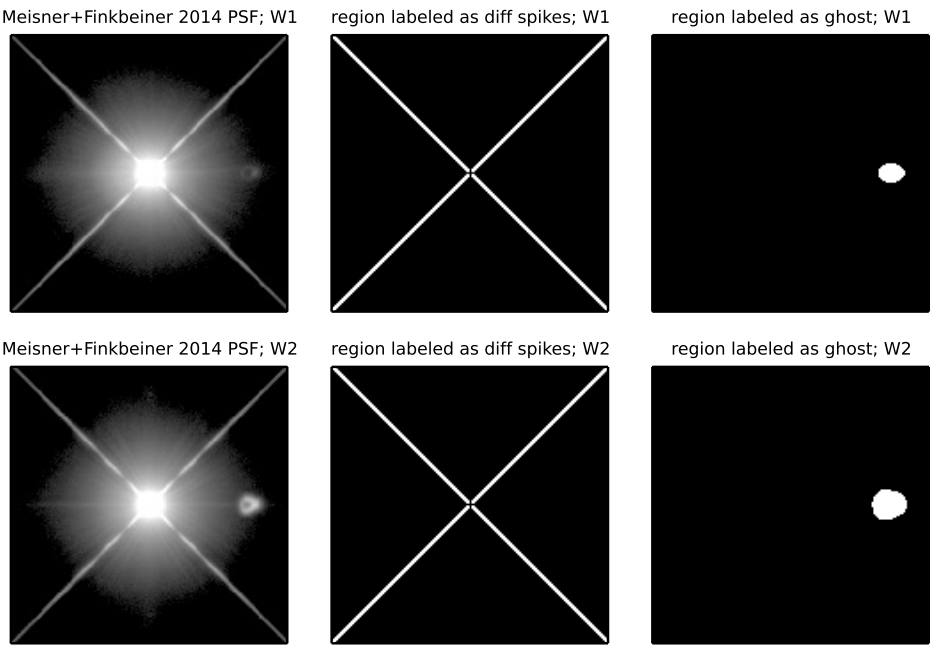

Figure 2: The PSF models used for creating our unWISE bitmasks, alongside corresponding boolean masks labeling PSF regions containing diffraction spikes and optical ghosts. Each subplot is $14.9'$ on a side. Top left: W1 focal plane averaged PSF model. Top center: regions of the W1 PSF model labeled as containing diffraction spikes are shown in white on an otherwise black background. Top right: W1 PSF region labeled as being affected by an optical ghost. Bottom left: W2 focal plane averaged PSF model. Bottom center: regions of the W2 PSF model labeled as containing diffraction spikes. The top and bottom panels in the middle column are identical. Bottom right: W2 PSF region labeled as being affected by an optical ghost. The optical ghost is much more prominent in W2 than in W1.

0-3, we use the ghost regions labeled in the right column of Figure 2 to keep track of which pixels fall within bright source ghosts. We then generate our ghost-specific mask bits (11-12 in W2 and 25-26 in W1) by flagging those pixels that are within ghost-affected regions and have model surface brightnesses larger than $\Gamma_{ghost} = 0.15\Gamma$, where Γ is defined in Equation 1. In other words, we apply a *fainter* surface brightness threshold for masking within regions affected by ghosts, and assign the results of this modified thresholding to ghost-specific mask bits.

10 Bits 13-20: latent

Persistence artifacts referred to as "latents" within the WISE documentation are present in W1 and W2 imaging. When a bright source is imaged and saturates one or more WISE pixels, the sky location imaged by those same detector pixels in subsequent exposures will display a diffuse blob-like latent feature. Latents are more pronounced in W1 than W2, and therefore tend to appear as somewhat blue smudges (see Figure 3). Exceptionally bright stars can cause latents that remain noticeable for many exposures while decaying in amplitude over time. We refer to the number of exposures since imaging of the parent bright source as the "order" of a latent. Currently, our unWISE masking accounts for only first and second order latents i.e., those arising one and two exposures subsequent to imaging of the parent bright source. Because WISE scans at $\sim 0.7^\circ$ per exposure, the sky position of a latent is significantly offset from its parent source along the scan direction. This makes unflagged latents particularly troublesome for rare object searches — latents are difficult to trace back to their parent bright sources by eye, and can also be misinterpreted as flux variable or moving objects because they appear at different sky locations during different WISE sky passes which have differing scan directions. Latent positions are deterministic, and could all be predicted exactly given the WCS and timestamp of every exposure in combination with a perfectly accurate bright source catalog.

As a first step toward creating image-level unWISE latent masks, we generate a catalog of latents appearing in

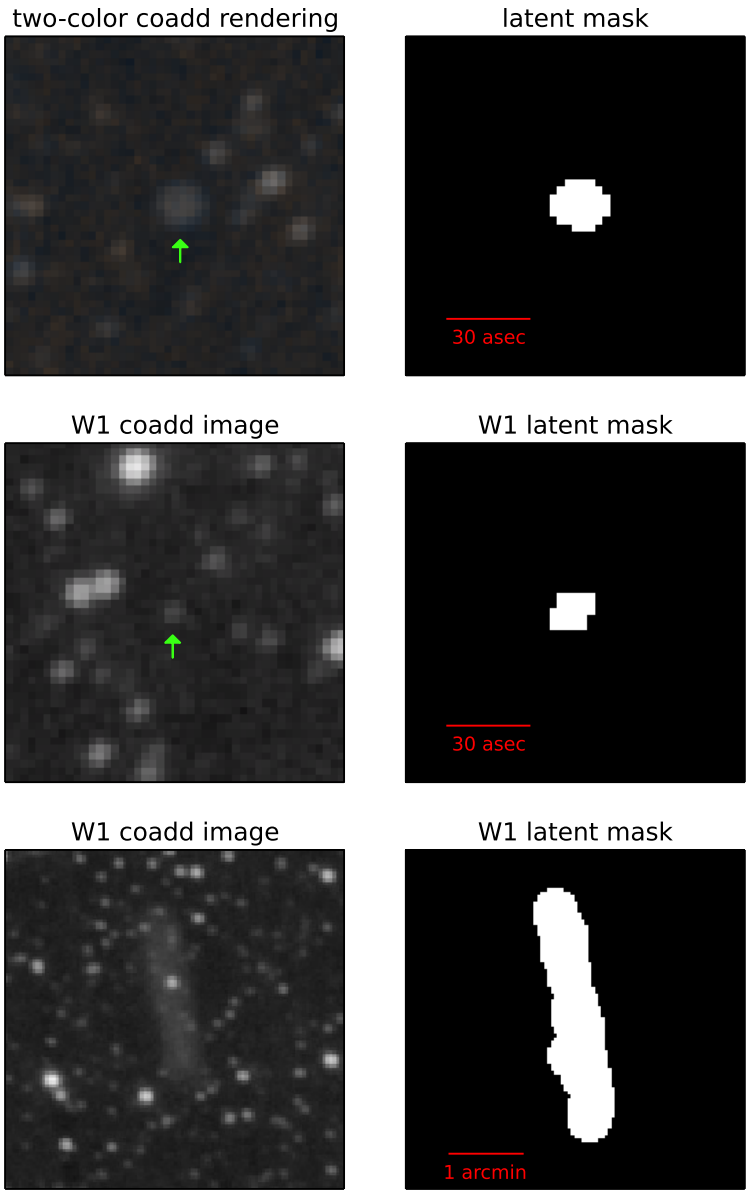

Figure 3: Examples of first order latents as imprinted on the unWISE coadds (left column) and flagged in our corresponding latent masks (right column). Top row: first latent of a $\sim$ 5th magnitude parent source, pointed to by a green arrow. The two-color composite at left displays W1 as blue and W2 as orange. This example illustrates the slightly blue appearance of latents relative to sources with typical color of W1$-$W2 $\approx$ 0. At right is a rendering of our unWISE bitmask in this latent's vicinity, with white pixels indicating that one or more of bits 13-16 is set. The location and size of the masked region match the observed artifact well. Middle row: W1 first latent of a `w1mpro` $\approx$ 8 parent source, which is close to the minimum brightness necessary to produce a latent. This latent covers a smaller region than does the first latent with $\sim$5th mag parent. Accordingly, a smaller region is flagged as affected by a W1 first latent, with white pixels at right indicating that bit 13 or 14 is set. Bottom row: latent arc produced by WISE scan direction variation at high absolute ecliptic latitude ($\beta \approx -76°$). In this case the parent is a $\sim$ 2.5 mag star. The region flagged as affected by W1 first latents traces this arc, appearing to overflag somewhat as shown at right.

each unWISE tile footprint and each band. To make the computation of latent positions within each coadd efficient, we precompute per-band lookup tables containing the MJDs and full WCS parameters of all ∼25 million single-exposure W1/W2 images. For each unWISE tile footprint in each band, we use the unWISE `-frames` metadata table to determine the list of exposures contributing to the corresponding full-depth coadd. We then loop over these exposures, combining our WCS/MJD lookup table and bright source list (§1) to determine the (RA, Dec) positions of latents appearing in each contributing exposure. We aggregate these latent world coordinates on a per-coadd basis, and convert this list of (RA, Dec) coordinates to pixel coordinates within the coadd under consideration. The result is one latent catalog per unWISE tile per band. In addition to world and coadd pixel coordinates, each such catalog contains a variety of metadata that will enable us to subsequently render image-level latent bitmasks. These metadata include, for each latent, the parent bright source magnitude, the WISE scan direction, and the latent's order (1 for first latent, 2 for second latent). In practice, when computing each coadd's catalog of latents, we do not analyze every single contributing exposure. Instead, we sort the contributing exposures by MJD and consider only every sixth exposure. This is done to reduce the computational cost of generating the latent catalog. Because a WISE sky pass typically includes $\gtrsim 12$ exposures at each sky location, and the WISE scan direction at a given sky position varies by $\lesssim 0.5^\circ$ over the time period of six exposures, analyzing only the latents from every sixth exposure should not cause any image-level under-flagging downstream.

Only a subset of the objects within our bright source list are sufficiently bright to create latents. Table 2 provides the magnitude thresholds that we employ for determining which bright sources are capable of causing first and second latents in each band. These thresholds are applied directly to the `w?mpro` values in our bright source list, and are taken to be constant over time and across the entire sky.

Table 2: Latent parent magnitude thresholds.

band	1^{st} latent threshold (mag)	2^{nd} latent threshold (mag)
W1	8.3	6.2
W2	7.0	4.9

To determine the angular size of the region that should be masked around each single-exposure latent location, we define an effective parent magnitude ($m_{eff,l}$) that takes into account several factors: the parent bright source's magnitude, the ecliptic latitude and the background level. The following terms contribute to the determination of $m_{eff,l}$:

$$\Delta_{bg,l} = f_{bg,l} \cdot log_{10}\Big[max(intmed/intmed_0, 1)\Big] \tag{2}$$

$$\Delta_{arc,l} = 2.5 \cdot log_{10}(max(\delta\theta, \delta\theta_0)/\delta\theta_0),\ \delta\theta_0 = 1^\circ \tag{3}$$

The effective parent magnitude used to compute the size of each single-exposure latent is then:

$$m_{eff,l} = m + \Delta_{bg,l} + \Delta_{arc,l} \tag{4}$$

Where m is the parent source's `w?mpro` value taken from our bright source list. *intmed* is the sky background level in WISE L1b DN. This sky background level is computed for each band on a per unWISE tile basis, by taking the median of the `intmedian` values in the unWISE `-frames` metadata table, restricted to frames that actually contributed to the coadd. The *intmed* value used in Equation 2 is that of the unWISE tile for which the bitmask image is being generated. $intmed_0$ is a fiducial background level appropriate at high Galactic latitude and low ecliptic latitude. In Equation 2, we adopt $intmed_0$ values of 26.5 (62.5) in W1 (W2). The $f_{bg,l}$ prefactor is set to 2.38 (3.78) in W1 (W2), and $\Delta_{bg,l}$ is capped at 4.3 magnitudes. We use $\Delta_{bg,l}$ to account for the fact that an increased background level tends to reduce the region over which a latent's profile is non-negligible.

$\Delta_{arc,l}$ accounts for reduced latent surface brightness in the unWISE coadds due to increased arcing of latent imprints as $|\beta|$ becomes larger (see bottom row of Figure 3). Because of the continuous variation of the WISE scan direction at high ecliptic latitude, the coadd-level imprint of a bright source's multiple single-exposure latents is spread across an area which is $\sim \delta\theta/\delta\theta_0$ larger than it would have been in the ecliptic plane, with $\delta\theta$ given by:

$$\delta\theta = 0.78^\circ/cos(\beta) \tag{5}$$

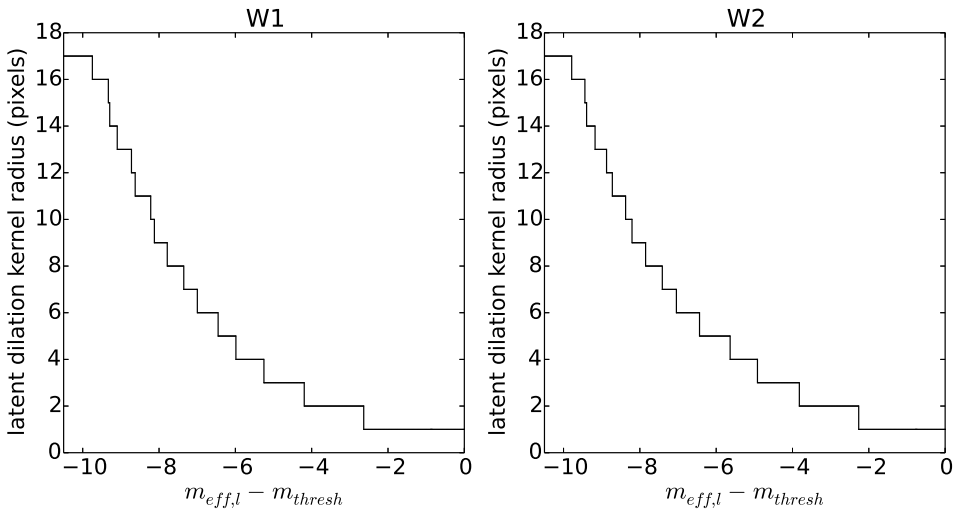

Figure 4: Radius of per-latent circular binary dilation kernel as a function of difference between the effective parent magnitude of the latent (Equation 4) and the latent parent magnitude threshold (Table 2). Left: W1. Right: W2. The radius is always floored at 1 pixel (corresponding to a 3×3 pixel rectangular dilation kernel), and capped at 17 pixels. For a given WISE band and order of latent, the region affected becomes larger as the parent's effective magnitude decreases. The increase of our adopted dilation radius toward lower $m_{eff,l}$ captures this behavior.

Equation 5 can be thought of as the range of ecliptic longitude spanned by a WISE exposure (0.78° on a side), as a function of ecliptic latitude. This approximately corresponds to the range of ecliptic pole approach angles sampled as a function of β. $\delta\theta_0$ is set to 1° because this is the approximate ecliptic pole approach angle spread within a given scan parity (northward or southward) for regions near the ecliptic plane. $\delta\theta$ must be capped at 180°, at which point latents will have been spread out into complete rings surrounding their parent stars[4]. Note that β in Equation 5 refers to the location of the parent bright source.

To flag pixels affected by latents in a given unWISE coadd footprint, we begin by using nearest neighbor interpolation to mark each pixel corresponding to a single-exposure latent listed in the relevant latent catalog and having $m_{eff,l} \leq m_{thresh}$, where m_{thresh} is the magnitude threshold for the type of latent being considered (see Table 2). We then apply a binary dilation about each of these marked pixels using a circular kernel, with a radius that depends on the difference $(m_{eff,l} - m_{thresh})$. Figure 4 shows the dilation radius in pixels as a function of $(m_{eff,l} - m_{thresh})$. We determined the shape of this function by assuming that for a parent source of magnitude m_{thresh}, only the centermost pixel of the profile is sufficiently saturated to yield a non-negligible latent imprint. Then, using the Meisner & Finkbeiner (2014) PSF model profile, we determined the radius of saturation that would result from making the total parent flux larger by $10^{-(m_{eff,l}-m_{thresh})/2.5}$.

As listed in Table 1, there are eight unWISE mask bits for latents, one for each possible combination of WISE band (W1 or W2), scan direction (north or south), and latent order (first or second). Currently, our latent masking is based on latent catalogs generated before we had incorporated 2MASS K_S information into our bright source list as described in §1. In the future we will attempt to remedy this inconsistency with other unWISE mask bits by regenerating our latent catalogs based on the latest version of our bright source list. In future iterations of our latent catalogs, we may compute latents for every exposure as opposed to every sixth exposure despite the larger computational cost. Lastly, in future versions of our unWISE bitmasks, we may incorporate latents of exceptionally bright stars beyond second order.

11 Bits 21-22: bright source centroid

Many unWISE mask bits associated with bright sources flag the location of the parent bright source itself, a feature which may at times be considered undesirable. To address this situation, mask bit 21 (22) marks a 3×3 pixel box

[4]This consideration is only relevant over a tiny portion of the sky, $|\beta| > 89.75°$.

surrounding the centroid of each object in the W1 (W2) bright source sample described in §1.

12 Bits 23-24: AllWISE-like circular bright source halo

In order to offer a set of unWISE mask bits similar to the AllWISE CC flags, we include bits flagging circular "halos" around bright sources. We attempt to use an AllWISE-like approach for creating our circular halo masks. Bit 23 (24) flags circular halos around bright sources in W1 (W2). Our halo radius formula, adapted from that of AllWISE, depends on the parent source's brightness, the sky background level, and absolute ecliptic latitude. The sky background level is relevant because the halos of bright stars become negligible at smaller radii when the sky background is higher, for example in the Galactic plane. The WISE coverage increases toward the ecliptic poles, so that for fixed parent star brightness and sky background level, the halo will tend to be appreciable relative to typical pixel noise out to a larger radius at higher absolute ecliptic latitude.

To construct our sample of halo parent sources, we downselect the bright star sample of §1 to sources with `w?mpro` < 8 in the relevant band[5]. We then use the following formulae to determine the halo radius, in arcseconds:

$$r_h = B \cdot 10^{a \cdot m_{eff,h} + b} \tag{6}$$

$$B = c_{bg} \cdot log_{10}(intmed) + d_{bg},\ B_{min} \leq B \leq B_{max} \tag{7}$$

$$m_{eff,h} = m - 2.5 \cdot log_{10}\left[\sqrt{120/max[cos(\beta), 0.2]}\right] \tag{8}$$

The parameters of these equations are provided in Table 2. m is the `w1mpro` (`w2mpro`) value from our bright source list for W1 (W2). β is ecliptic latitude. For each halo parent source, the *intmed* background level of the nearest tile center is adopted (see §10 for a description of how per-tile *intmed* values are calculated). $m_{eff,h}$ is an "effective magnitude" appropriate for use in the halo radius computation given the values of the other parameters. $m_{eff,h}$ is brighter than m by an offset which tracks the signal-to-noise increase of a fixed flux source as its ecliptic latitude, and therefore WISE coverage, increases[6]. The halo radius parameters were tuned based on inspection of five-year "NEO4" unWISE coadds – different halo radii may be preferable when deeper or shallower unWISE coadds are being analyzed. Our halo radius functional forms and parameters are substantially rooted in those used by ARTID. Figure 5 shows our halo radii as a function of parent magnitude at $\beta = 0$ and with fiducial high Galactic latitude sky background levels.

Table 3: Halo radius parameters.

band	a	b	c_{bg}	d_{bg}	B_{min}	B_{max}
W1	-0.144	2.76	-0.57	1.10	0.3	1.1
W2	-0.144	2.76	-1.35	2.30	0.3	1.1

At high Galactic latitude ($|b_{gal}| > 18°$), the typical fraction of area flagged by the unWISE circular halo masks is 1.2% (0.7%) in W1 (W2). We caution that circular masks are likely better implemented at the catalog level than at the image level, although image-level halo bitmasks do allow end users to conveniently dilate the halos as desired. Within each unWISE tile footprint, halos due to parent bright sources with centroids falling outside of the tile boundaries are always handled correctly.

13 Bits 27-28: PSF-based diffraction spike

Given the spatial extent of the PSF models we employ, we can use our PSF thresholding approach to make "PSF-based" diffraction spike masks out to a radius of up to $\sim 10.5'$. The methodology for doing so is analogous to that described in §9 for generating ghost-specific mask bits. We track which pixels in our bright source only models are

[5]This requirement is an attempt to mirror the `w?mpro` < 8 cut documented in item vi.2 of `http://wise2.ipac.caltech.edu/docs/release/allsky/expsup/sec4_4g.html`.

[6]The WISE frame coverage scales like $1/\cos(\beta)$, only deviating from this trend very nearby the ecliptic poles.

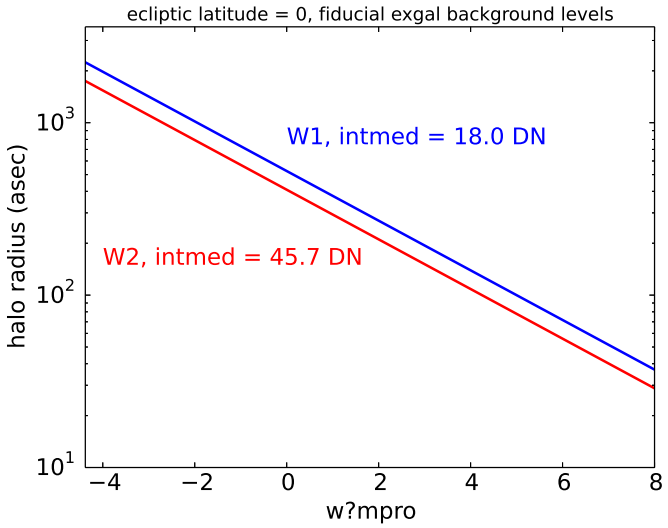

Figure 5: unWISE bitmask circular halo radii as a function of magnitude at $\beta = 0$ and with fiducial high Galactic latitude sky background levels.

within diffraction spikes, based on the PSF regions labeled in the center column of Figure 2. Within these diffraction spike regions, we apply a reduced brightness threshold of $\Gamma_{spike} = 0.05\Gamma$, thereby generating mask bits specific to the diffraction spikes (bit 27 in W1 and 28 in W2). Because the WISE diffraction spikes are quite nearly symmetric under 180° rotation, the northward and southward scan direction diffraction spike masks are virtually identical. We therefore do not report PSF-based diffraction spikes using separate mask bits for each scan direction. Instead, each band's PSF-based diffraction spike bit is the OR of PSF-based diffraction spike flagging computed in the two scan directions.

14 Bits 29-30: geometric diffraction spike

Diffraction spikes are captured to some extent in bits 0-3, and to a large extent in bits 27-28. However, for sufficiently bright stars (`w?mpro` $\lesssim 6$), the diffraction spikes can reach beyond the boundaries of the Meisner & Finkbeiner (2014) W1/W2 PSF models, which are limited to $\sim 15'$ on a side. To handle such situations, we have implemented geometric diffraction spike mask bits for `w?mpro` $\lesssim 6$ sources, extending up to $\sim 1.5°$ from the parent's centroid.

Our geometric diffraction spike masks consist of straight lines emanating outward from the bright source centroid at angles of 45°, 135°, 225°, and 315° from ecliptic north. In a manner similar to that used for determining circular halo size (§12), we account for multiple factors when computing the geometric diffraction spike length: the parent source brightness, the sky background level, and the absolute ecliptic latitude. These factors are taken into account by computing an "effective magnitude" ($m_{eff,sp}$) for each object in our bright source sample. The following are terms that contribute to our computation of $m_{eff,sp}$:

$$\Delta_{bg,sp} = 2.5 \cdot log_{10}\Big[max(intmed, intmed_0)/intmed_0\Big] \tag{9}$$

$$\Delta_{cov,sp} = -2.5 \cdot log_{10}\Big[\sqrt{1/cos(min(\beta, 80°))}\Big] \tag{10}$$

The effective magnitude is then computed as:

$$m_{eff,sp} = m + \Delta_{bg,sp} + \Delta_{cov,sp} + \Delta_{fl,sp} \tag{11}$$

Where m is the `w1mpro` (`w2mpro`) value from our bright source list in W1 (W2). We only generate geometric diffraction spike masks for bright sources with $m_{eff,sp} < 6$. $\Delta_{bg,sp}$ is a penalty that increases a bright source's magnitude (makes it considered to be effectively fainter) in regions of relatively high background. *intmed* is the

sky background level in WISE L1b DN, defined the same way as in our latent effective magnitude computation. When computing geometric diffraction spike radii, we floor *intmed* at a fiducial extragalactic, low ecliptic latitude value $intmed_0$, taken to be 25 DN (60 DN) in W1 (W2). This forces $\Delta_{bg,sp}$ to be a strictly non-negative correction. $\Delta_{cov,sp}$ acts to decrease a bright source's effective magnitude (make it be considered brighter) with increasing absolute ecliptic latitude. At higher $|\beta|$, WISE provides larger frame coverage and hence reduced background noise in the unWISE coadds. The functional form of $\Delta_{bg,sp}$ results in a correction that tracks the decrease in background pixel noise with ecliptic latitude. In computing $\Delta_{bg,sp}$, we cap this ecliptic latitude correction at its $|\beta| = 80°$ value, to avoid applying excessively large corrections very nearby the ecliptic poles.

At high ecliptic latitude, each unWISE coadd averages together frames with a significant spread in approach angles toward the ecliptic pole. Diffraction spikes therefore begin to take on a "flared" appearance at high $|\beta|$, and are ultimately washed out into nearly disk-like patterns in the immediate vicinity of the ecliptic poles. This results in decreased diffraction spike surface brightness at high ecliptic latitude, which we account for with the $\Delta_{fl,sp}$ term in Equation 11. The value of $\Delta_{fl,sp}$ is given by the right hand side of Equation 3. In the case of geometric diffraction spikes, $\delta\theta$ (given by Equation 5) is capped at 90° because the flaring of diffraction spikes will form a complete "disk" around bright stars once the spread in ecliptic pole approach angles reaches this value (due to the fact that the single-exposure WISE diffraction spikes emanate outward at azimuthal angles spaced at 90° intervals).

Analytic functions of $m_{eff,sp}$ determine the geometric diffraction spike radius for each bright source. These functional forms and parameters are substantially rooted in those used by ARTID. The geometric diffraction spike radius is given by:

$$r_{sp} = B_L \cdot 10^{a_L \cdot max(m_{eff,sp}, -2) + b_L} \cdot T(m_{eff,sp}) \tag{12}$$

$$T(m_{eff,sp}) = 1 - (6 - max(m_{eff,sp}, -2))/16 \tag{13}$$

r_{sp} has units of arcseconds and $T(m_{eff,sp})$ is a tapering function that modulates the ARTID-like prescription in Equation 12. Given that Equation 13 floors $m_{eff,sp}$ at -2 and is only applied for $m_{eff,sp} < 6$, we always have $0.5 \leq T(m_{eff,sp}) < 1$. $T(m_{eff,sp})$ ramps linearly with effective magnitude in the range $-2 \leq m_{eff,sp} < 6$. The parameters of Equation 12 are listed in Table 4, and the geometric diffraction spike radius as a function of effective magnitude is shown in Figure 6.

Table 4: Geometric diffraction spike radius parameters.

band	B_L	a_L	b_L
W1	10.0	−0.195	3.38
W2	10.0	−0.178	3.14

We initially mark geometric diffraction spikes as narrow, ∼1 pixel wide lines of the appropriate orientation and length. We then dilate these narrow versions of the geometric diffraction spike masks by an amount which depends on the parent bright source effective magnitude, dilating more aggressively for brighter parent sources. Specifically, we dilate with a 5 × 5 pixel square kernel for $m_{eff,sp} > 0$, a 9 × 9 pixel square kernel for $-2 < m_{eff,sp} \leq 0$, and a 13 × 13 pixel square kernel for $m_{eff,sp} \leq -2$.

Interior to each unWISE tile footprint, geometric diffraction spikes due to parent bright sources with centroids falling outside of the tile boundaries are handled correctly. Although we reduce the geometric diffraction spike radii to account for flaring at high $|\beta|$, this flaring is not reflected in the morphology of the regions masked. We hope to implement this functionality in a future release of the unWISE bitmasks; this limitation of the present bitmasks is only relevant over a small fraction of the sky near the ecliptic poles.

15 Collapsing scheme for DESI imaging and unWISE Catalog

For certain applications, the full content of the native unWISE bitmasks (Table 1) may be unnecessary. In particular, the splitting of artifacts into multiple bits based on scan direction is only relevant for time domain applications. Several catalogs which do not require scan direction dependent masking information already employ our unWISE bitmasks. Specifically, these are the unWISE Catalog and the DESI imaging surveys (Dey et al. 2018). For application to these catalogs, we have developed a scheme for collapsing the native 31-bit unWISE mask information

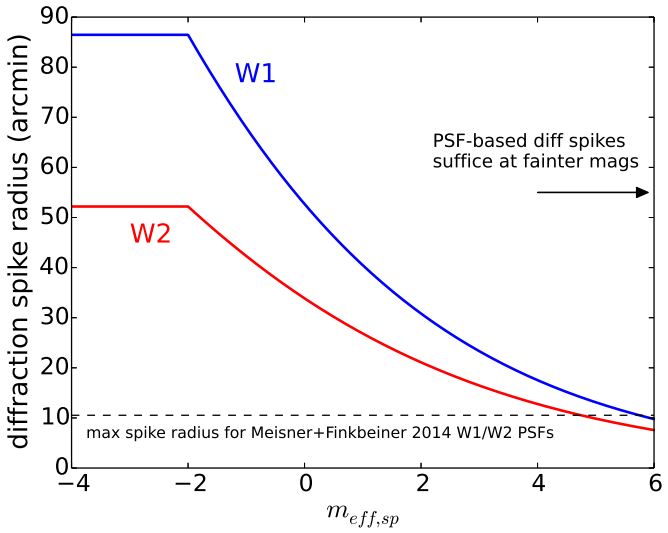

Figure 6: unWISE bitmask geometric diffraction spike radius as a function of effective magnitude, $m_{eff,sp}$. The blue (red) curve represents W1 (W2). The horizontal dashed black line is the maximum diffraction spike radius that can be accommodated within our PSF-based diffraction spike masking described in §13. This figure shows that the effective magnitude at which our geometric diffraction spike masking goes into effect ($m_{eff,sp} = 6$) coincides approximately with the effective magnitude at which the PSF-based diffraction spike masking can no longer be adequate.

Table 5: Collapsing of unWISE mask bits for DESI imaging and unWISE Catalog

Summary Bit	meaning	native unWISE bit logic (W1)	native unWISE bit logic (W2)
0	bright star core and wings	0 OR 1	2 OR 3
1	PSF-based diffraction spike	27	28
2	optical ghost	25 OR 26	11 OR 12
3	first latent	13 OR 14	15 OR 16
4	second latent	17 OR 18	19 OR 20
5	AllWISE-like circular halo	23	24
6	bright star saturation	4	5
7	geometric diffraction spike	29	30

into a smaller number of summary bits. The definitions of our 8 summary bits in terms of the native unWISE mask bits of Table 1 are provided in Table 5. The unWISE bitmasks are also being used by CatWISE, but with a different prescription for mapping the native unWISE mask bits to AllWISE-like character strings that encode the types of artifacts affecting each source.

16 Other possible future improvements

In the preceding sections, we have suggested a number of detailed improvements we may implement in the future. In this section we mention a few additional upgrades that could be also be implemented.

- More finely pixelized bitmasks — The unWISE bitmasks are pixelized at the native WISE pixel scale of $2.75''$/pixel. Each such pixel covers an area equivalent to > 100 pixels of optical data from the DESI imaging MzLS and DECaLS surveys. Thus, our current pixel size may limit the utility of applying our masks to WISE forced photometry based on detections in much higher resolution optical imaging. To address this, we could generate the unWISE bitmasks using a smaller pixel size.
- W3 and W4 — In the future we could include information about W3 and W4 in our unWISE bitmask products.

- Nebulosity — Nebulosity due to Galactic dust can be problematic for source detection and modeling analyses. The unWISE Catalog processing uses a neural network to classify whether or not a sky region is affected by nebulosity (Schlafly et al. 2018), and reports this information via the `flags_info` image product. This nebulosity flagging could potentially be added into the main unWISE bitmask images.
- Overflagging in the Galactic plane — Despite our efforts to limit masking in high source density regions, some mask bits still flag excessively large fractions of area in parts of the Galactic plane, mostly toward the Galactic center. Further tuning of the ways in which masking is scaled based on source density and sky background level could be attempted.
- Homogenizing procedures for different mask bits — More work could be done to homogenize the separate procedures used to create different unWISE mask bits. For example, our PSF thresholding scales back masking in crowded regions based on a map of Gaia source density, whereas the geometric and latent mask bits do so based on sky background level.

References

Dey, Schlegel, Lang et al. 2018, arXiv:1804.08657
Gaia Collaboration et al. 2018, A&A,616, 1
Makarov et al. 2014, A&A, 570, 13
Meisner, Bromley, Nugent et al. 2017b, AJ, 153, 65
Meisner & Finkbeiner 2014, ApJ, 781, 5
Meisner, Lang & Schlegel 2017a, AJ, 154, 161
Schlafly et al. 2018, ApJS, 234, 39
Schlegel, Finkbeiner & Davis 1998, ApJ, 500, 525